Anadolu Üniversitesi Bilim ve Teknoloji Dergisi A- Uygulamalı Bilimler ve Mühendislik
Anadolu University Journal of Science and Technology A- Applied Sciences and Engineering

2016 - Volume: 17 Number: 5
Page: 812 - 822
DOI: 10.18038/aubtda.279850
Received: 08 August 2016 Revised: 05 October 2016 Accepted: 01 November 2016

MECHANICAL, ELECTRICAL AND THERMAL PROPERTIES OF α/β SiAlON-SiC COMPOSITES FABRICATED BY GAS PRESSURE SINTERING METHOD

Erhan AYAS *

Department of Materials Science and Engineering, Anadolu University, Eskişehir 26555, Turkey

ABSTRACT

α/β SiAlON-SiC composites were produced by coating SiAlON based spray dried granules with varying amounts of SiC (0-10 vol % SiC) following gas pressure sintering technique. A two step sintering schedule between 1940-1990°C under 10 MPa N_2 gas pressure was adopted in order to achieve high densification rate. All the composites and the reference SiAlON material were densified up to 99 %. α/β SiAlON - 10 vol. % SiC composite had the highest hardness value (Hv10: 16.33 GPa) due to the formation of α-SiAlON phases promoted with the increasing SiC content. No significant changes in the fracture toughness values of composites were observed. 3D segregated network of SiC particles along granules to establish electrical and thermal conductivity in the composites was successfully achieved with incorporation of 10 vol. % SiC. α/β SiAlON - 10 vol. % SiC composite exhibited the semiconductor characteristic and high thermal conductivity with the electrical resistivity of 10^2 Ω.m and thermal diffusivity of ~11 mm^2/s measured at room temperature.

Keywords: SiAlON; SiC; Electrical conductivity; Thermal conductivity, Gas pressure sintering (GPS)

1. INTRODUCTION

SiAlONs have attracted much attention so far as non-oxide engineering ceramics owing to their outstanding combination of high mechanical and thermal properties which they possess both at room and high temperature. These materials have been in use generally for structural engineering applications including cutting tools, mechanical seals, bearings, heat exchangers and components for heat engines [1]. In order to broaden the application areas, the incorporation of particulate second phase into ceramic matrixes, the most common method, could be used by using composite approach. As a reinforcement agent, nitrides (TiN) [2, 3], carbides (SiC) [4], carbonitrides (TiCN) [1, 5], borides (TiB_2) [6], and silicides ($MoSi_2$) [7, 8], enhances the electrical conductivity which has allowed the use of these materials as igniters, glow plugs and heaters [1].

Among these, SiC particles are most widely incorporated into the α/β-SiAlON matrixes due to the match of expansion coefficient and density between Si_3N_4 and SiC (α = 3.4 x $10^{-6}K^{-1}$ and ρ ~ 3.3 g/cm^3 for Si_3N_4; α = 4.3 x $10^{-6}K^{-1}$ and ρ ~ 3.2 g/cm^3 for SiC). It is known that SiC is one of the hardest known materials [9]. Furthermore, the incorporation of sub-micron SiC particles into α/β-SiAlON matrixes results in the production of composites with not only excellent hardness but also improved bending strength [10, 11]. With this particular approach, high amounts (30–40 vol. %) of such secondary phases must be employed to achieve desired conductivity value. However, such large additions usually cause a non-uniform and agglomerated dispersion leads to the degradation of some of the important properties of the matrix material. On the other hand, the densification of this type of composites with conventional techniques has been found very difficult due to covalent nature of these phases and undesirable reactions between constituents. Hot pressing (HP) and hot isostatic pressing (HIP) are generally preferred for commercial products. However, costly and time consuming secondary machining processes are required following the basic form of a workpiece is created. To overcome above stated problems, the amount of secondary phase addition must be minimized.

*Corresponding Author: erayas@anadolu.edu.tr

In the segregated network concept, it is possible to achieve high electrical conductivity with a very low conductive phase content by creating a continuous network of conductive particles at the interface between grains of the insulating matrix phase. Electrical conductivity of this type of composites dramatically increases by several orders of magnitude after a critical value of filler concentration, known as the percolation threshold. For the emphasized purpose for the perfect composite structure involved spherical shaped particles, coating a spherical particle with a conductive phase could be an innovative approach [12 -17].

It is known that gas pressure sintering (GPS) technique has advantageous effects such as prevention of pore formation, promoted densification behavior and minimize the content of oxide additives due to high-pressure nitrogen suppresses [18, 19]. The sintering of SiC reinforced α/β-SiAlON composites by GPS has been studied before [9, 20-22]. Though, to the best of our knowledge, no study based on the investigation of influence of segregated network on both electrical and thermal conductivity in α/β-SiAlON/SiC composites has been conducted. Thefore, in this study, SiAlON based granules were prepared by spray drying and coated with nano SiC particles in varying amounts (0-10 vol.%) using a dry mixing process in an attempt to form of a segregated network. The densification behavior and mechanical, electrical and thermal properties of the reinforced composites were compared with monolithic SiAlON matrix.

2. MATERIALS AND METHODS

2.1. Preparation of SiC Coated SiAlON Composites

Spray dried SiAlON granules were supplied by MDA Advanced Ceramics Ltd. (Eskisehir/Turkey). The composition was designed to provide 25% α-SiAlON / 75% β -SiAlON in the final product. In order to prepare α–β SiAlON composition (designated as SN), 89.4 wt% Si_3N_4 (SN-E10, Ube Industries Ltd., Japan), 5.4 wt% AlN (HC Starck GmbH, Germany), 2.5 wt% Al_2O_3 (Sumitomo, Japan), 4.73 wt% Y_2O_3 (Shin Etsu Chemical Co., Ltd., Japan), 0.4 wt% Sm_2O_3 (Sigma–Aldrich, Germany) and 0.12 wt% $CaCO_3$ (Riedel-de Haën, Germany) were used as starting powders. The powders were mixed through attrition milling with de-ionized water as liquid media and Si_3N_4 grinding balls for 2 h in a polyamide container. The slurry was then dried in a spray drier (Nubilosa, Germany) to obtain spherical granules of around 100 μm in diameter, under suitable conditions. Monolithic SiC powder (99.9% purity, H. C. Starck, Germany) with the particle size of 75 nm and spesific surface area of 23-26 m^2/g was used as coating material. For the coating process, appropriate amounts of SiAlON granules and SiC powder (0, 2.5, 5, 7.5 and 10 vol.%) were weighted and dry mixed by using a classical ball mill device with a rotational speed of 30 rpm for 24 h in a plastic container under RT conditions.

2.2. Shaping and Gas Pressure Sintering (GPS)

Sintering of the pellets was carried out in a BN crucible using a GPS furnace (FCT Systeme GmbH, Germany), capable of operating at temperatures of up to 2000°C in N_2 and Ar atmosphere of up to 10 MPa. A two-stage sintering schedule was employed. The first stage of sintering was accomplised at 1940°C for 60 min under a N_2 gas pressure of 0.2–0.5 MPa. In the second stage, both the peak temperature and gas pressure were raised to 1990°C and 10 MPa, respectively, for the same soaking time. The heating and cooling rates were kept at 10°C/min.

2.3. Characterisation

Following the removal of h-BN reacted surface, relative densities of the samples were measured in distilled water by the Archimedes method. Phase identification was performed on ground powder samples using XRD (Rigaku Rint 2200-Japan) with Ni-filtered Cu Kα radiation. Intensities of the

(1 0 2) and (2 1 0) peaks of the α–SiAlON phase and the (1 0 1) and (2 1 0) peaks of the β-SiAlON phase were used for quantitative estimation of the α:β phase ratio [23]. Both granule surfaces before and after coating and polished surfaces of the sintered samples were examined under SEM (FESEM, Supra 50 VP, Zeiss-Germany). Vickers hardness (Hv_{10}) from the polished surfaces of the sintered samples was measured by using an indenter (Emco-Test, M1C, Germany) with a load of 10 kg. The fracture toughness (K_{IC}) of the samples was evaluated from the radial cracks formed during the indentation test. The K_{IC} values are calculated according to the Anstis formula [24]. Electrical resistivity measurements were carried out by using two probe method at room temperature on the disc shape samples. Au electrodes were deposited on the both sides of the samples. The volume resistivity of the composites was measured by using a Keithley 6517A Electrometer/High resistance meter. Thermal diffusivity measurements were performed by using a Netzsch LFA-457 Laser-Flash system in the temperature range of 20-600°C under N_2 gas atmosphere. Au electrodes were deposited and then carbon were sprayed on the both sides of samples.

3. RESULTS AND DISCUSSION

Properties of the investigated composites are given in Table 1. The relative density values of SN – 0 vol % SiC, SN – 2.5 vol % SiC and SN – 5 vol % SiC composites were found equal to 99.9%. With the increment of SiC content, the relative density value of SN – 7.5 vol % SiC composite decreased to 99.4% and this value was further decreased down to 98.8% for SN – 10 vol % SiC composite. No closed porosity was observed during microstructural investigations. However, priory of sintering process, the aggregates in large sizes were detected with the increment of SiC content during the powder mixture process. The porosity formation of the investigated composites incorporated with 10 vol % SiC was demonstrated in Figure 1. It could be seen that the porosities were particularly located in the regions of aggregates. These formations decrease the densities of composites.

Table 1. Properties of the investigated composites

Composition	Bulk Density (g/cm^3)	Relative density (%)	α/β phase ratio	Hv_{10} (GPa)	K_{IC} ($MPa.m^{1/2}$)
SN	3.25	99.9	17 : 83	14.85 ± 0.14	5.86 ± 0.11
SN – 2.5 vol % SiC	3.25	99.9	23 : 77	14.83 ± 0.12	5.84 ± 0.04
SN – 5 vol % SiC	3.25	99.9	25 : 75	15.33 ± 0.20	5.90 ± 0.08
SN – 7.5 vol % SiC	3.23	99.4	31 : 68	15.78 ± 0.16	5.93 ± 0.05
SN – 10 vol % SiC	3.21	98.8	40 : 59	16.33 ± 0.23	5.98 ± 0.08

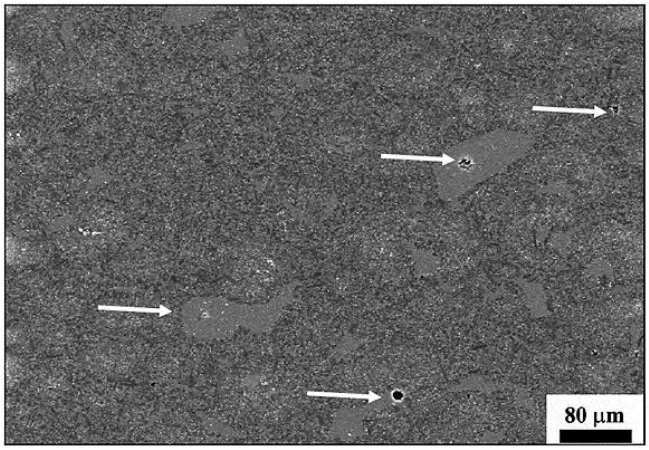

Figure 1. SEM image (SE mode) of the porosity formation in the investigated composites including 10 vol % SiC.

3.1. Phase and Microstructural Development

Representative X-ray diffraction patterns of the sintered samples coated with 0–10 vol % SiC are shown in Figure 2. α-SiAlON, β-SiAlON and SiC (6H) were detected as the major crystalline phases. The determined α-SiAlON and β-SiAlON phase ratios though XRD patterns were given in Table 1. Although the composition was designed to provide 25% α-SiAlON and 75% β-SiAlON, the α-SiAlON ratio of designed SN composition was determined 17 %. The α-SiAlON ratio of sintered SN – 10 vol % SiC at 1890°C-1940°C was determined 21 %. The reason of the decrease in α-SiAlON ratio on the monolitic SN ceramic attributed the promoting of α→β SiAlON transformation depends on the high sintering temperature. The amount of α-SiAlON phases for SN – 7.5 vol % SiC and SN – 10 vol % SiC composites was evaluated higher than the SN ceramic. On the other hand, as seen in the SEM image of SN – 10 vol % SiC (Figure 3), high amount of β-SiAlON grains exist particularly along the granule boundaries and β-SiAlON and α-SiAlON grains were located in granule cores. In the images the black colored elongated grains represent the β-SiAlON phase. The α→β SiAlON phase transformation was thought to have occurred more rapidly in these regions. Since no data is available for the oxygen content of the SiC powder, it was believed that the incorporation of surface oxygen originated from the SiO_2 phase had decreased the liquid phase formation temperature and affected the viscosity of the liquid phase which consequently accelerated the α→β SiAlON phase transformation. This additional SiO_2 increases the diffusion paths between reactive Si^{4+} and Al^{3+} species during sintering that restricts the formation of desired amount of β-SiAlON phase [26].

However Liu et al. [27] reported that the addition of SiC prevents α→β SiAlON transformation. Above-referred approach has supported by microstructıral investigations.

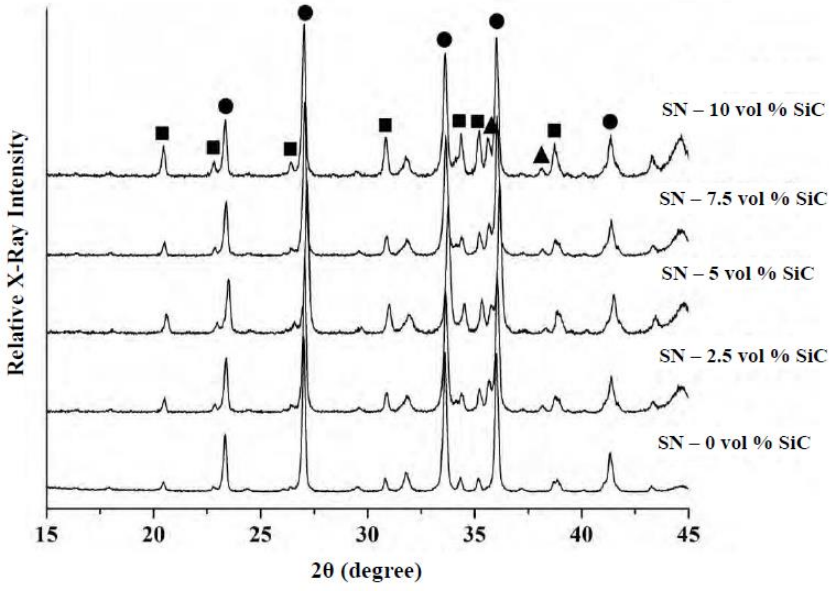

Figure 2. Representative X-ray diffraction patterns of the sintered samples coated with 0–10 vol % SiC. (■: α-SiAlON, ●: β -SiAlON, ▲: SiC (Moissanite 6H)).

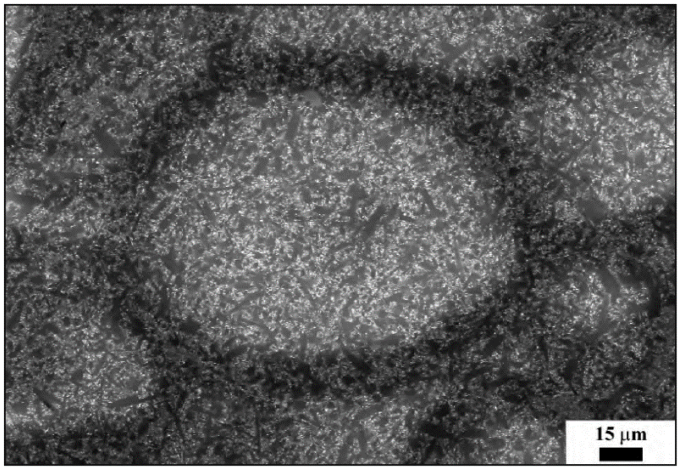

Figure 3. Representative SEM image of the β-SiAlON grains formed along the granule boundaries

Representative back scattered images of the investigated composites incorporated with 0-10 vol % SiC are given in Figure 4. SiC could not be distinguished at low magnifications due to the size of particles and also the close atomic number of SiC and formed SiAlON grains. With increasing amount of SiC, granule boundaries were more distiguishable in SEM images because of the existance of elongated β-SiAlON grains. It was more obvious for the SN – 7.5 vol % SiC and SN – 10 vol % SiC composites and it could be stated that SiC particles forms a 3D network. β-SiAlON grains along the granule boundaries appear darker than grains contained in the granule cores. It may be due to the thickness difference takes place during polishing. Furthermore, the formation of β-SiAlON grains in high amounts around the SiC particles was revealed with the high magnification images and agglomerated SiC particles during mixing were given in Figure 5. The aggregated SiC particles which have a size more than 100 μm were homogeneously sintered independently from the SiAlON matrix.

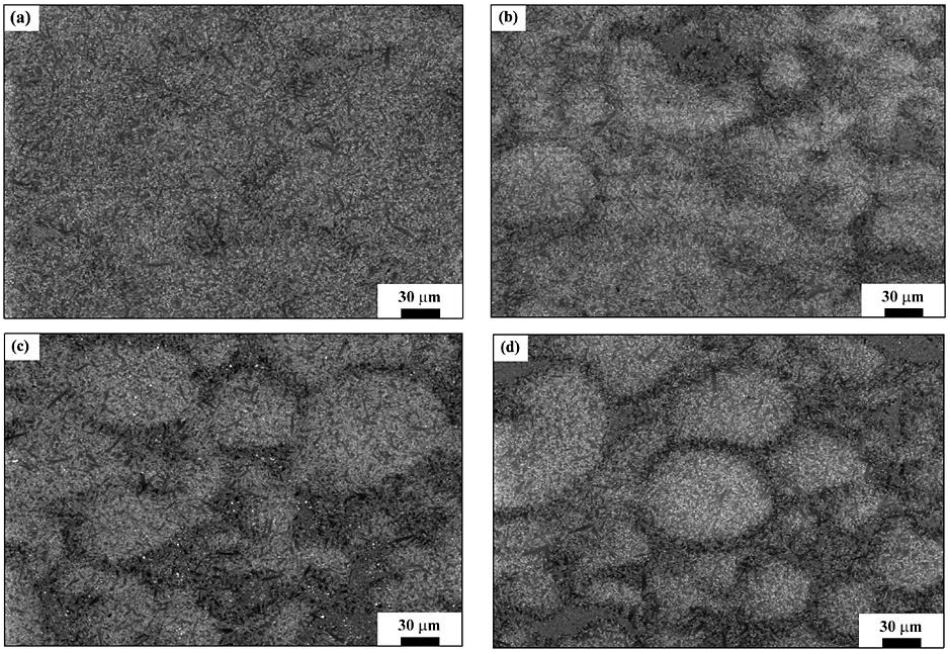

Figure 4. Representative back scattered images of the investigated composites incorporated with **(a)** 2.5 vol % SiC, **(b)** 5 vol % SiC, **(c)** 7.5 vol % SiC and **(d)** 10 vol % SiC.

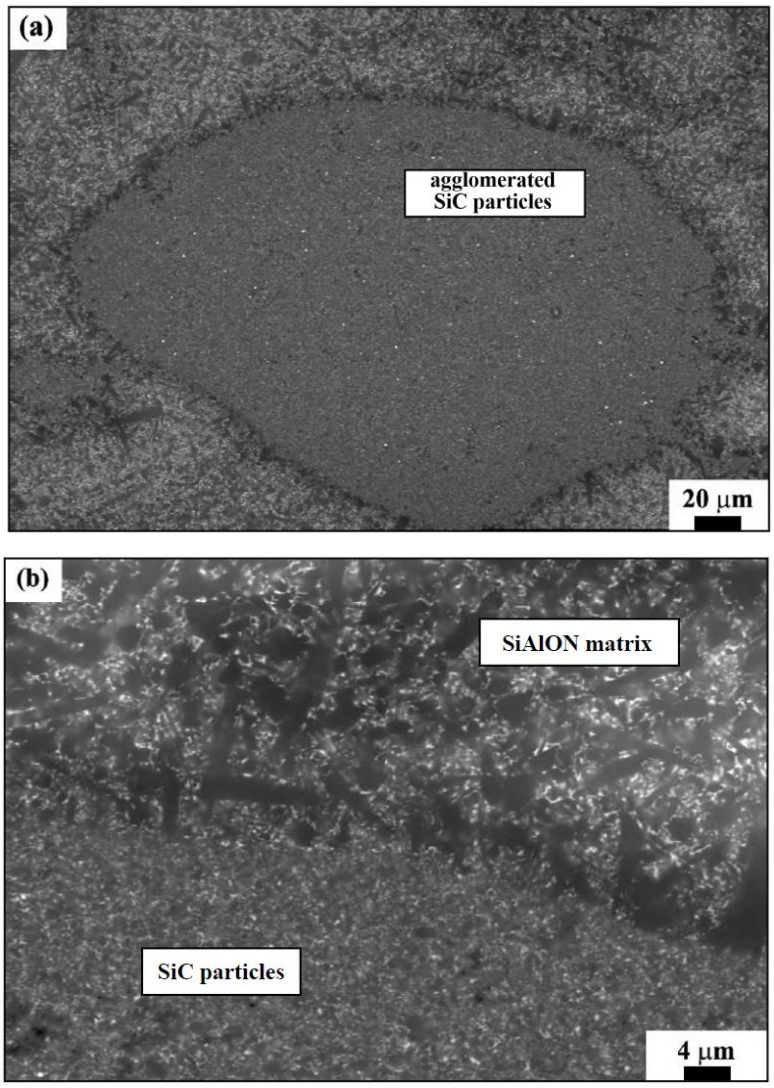

Figure 5. Representative SEM SEM image of the β-SiAlON grains formed around the SiC particles.

3.2. Mechanical Properties

Vickers hardness and the indentation fracture toughness of the composites are presented in Table 1. The hardness values of the composites increased with the enhancement of SiC content. As stated before that the formation of α-SiAlON phases was promoted with the increasing SiC content. Hence, the hardness of the composite SN – 10 vol % SiC which possessed the highest amount of α-SiAlON phase was found the highest value.

The fracture toughness values of composites were not strongly affected by SiC reinforcement. SEM images depicting the crack paths originated during Vickers indentation are given in Figure 6. The obtained β-SiAlON grains with high length/width ratio at high sintering temperatures have strong effect on the fracture toughness.

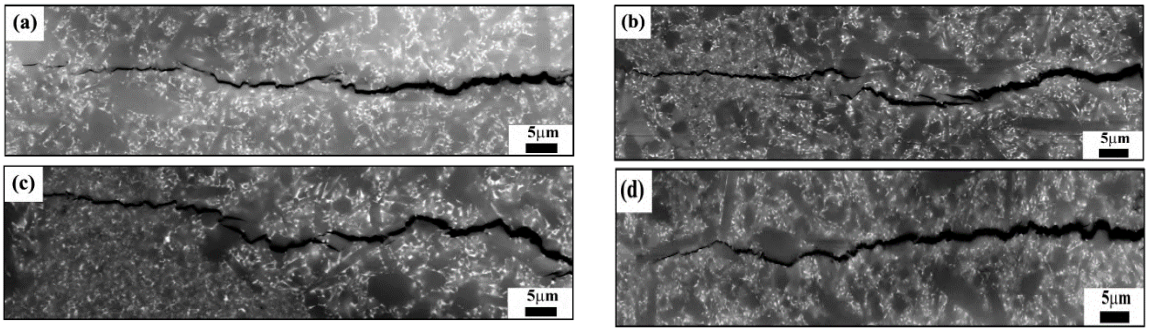

Figure 6. SEM images depicting the crack paths originated during Vickers indentation **(a)** SN - 2.5 vol % SiC, **(b)** SN - 5 vol % SiC, **(c)** SN - 7.5 vol % SiC and **(d)** SN - 10 vol % SiC.

3.3. Electrical Properties

The electrical resistivity values of the composites are plotted as a function of the SiC content in Figure 7. The electrical resistivity values of monolithic SN material and SN composites incorporated up to 7.5 vol. % SiC content are ~ $5x10^8$ - 10^{12} Ω.m, which is in the range expected from an insulator. The resistivity values of the SN composites decreased with the increasing of SiC amount. The resistivity value was further decreased down to ~ 10^2 Ω.m with 10 vol. % SiC confirming the semiconductor characteristic. It is reported that monolithic SiC has semiconductor characteristic with the electrical resistivity range of 10^{-3}-10^{-12} Ω.m [28].

The granule surfaces could not be well coated and no segregated network was observed with below 10 vol. % SiC due to formed SiC aggregates during mixing. According to the achieved results, a segregated network of SiC particles along granules was formed successfully for α–β SiAlON - 10 vol. % SiC, as reported segregated network concepts of α–β SiAlON–TiN and α–β SiAlON–TiCN composites [2, 25]. As mentioned in the microstructural development, the formation of β-SiAlON grains with high length/width ratio around SiC particles could be accepted as a reason to break SiC segregated network dependently the growth direction of grains.

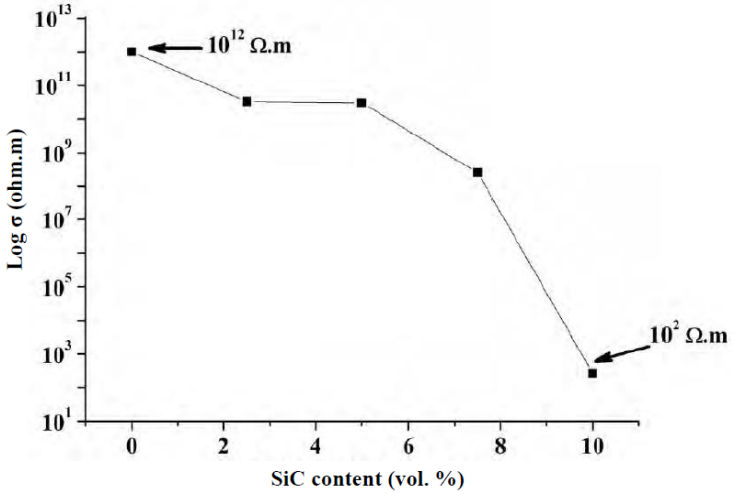

Figure 7. Change in the electrical resistivity of SN based composites with SiC content

3.4. Thermal Diffusivity

The thermal diffusivity values of investigated composites at room temperature are represented in Figure 8. The thermal diffusivity values were significantly increased with SiC content. The diffusivity value of the SN – 10 vol % SiC was found the highest value (~11 mm^2/s) regardless from temperature.

The reasons of increase in diffusivity values are twofold. With the increasing amount of SiC, particle-particle distance shortens and a 3D network of SiC grains in the composite microstructure developed. The shortening of the distance between the SiC grains promotes a tunneling effect for the conduction of phonons. Thus the thermal conductivity of SiC is higher than SiAlON phases. Secondly, elongated β-SiAlON grains that have better thermal conductivity than α-SiAlON grains on granule boundaries were formed in high quantity with the increase in SiC contentand assumed to be promote increase in the total thermal diffusivity of composites.

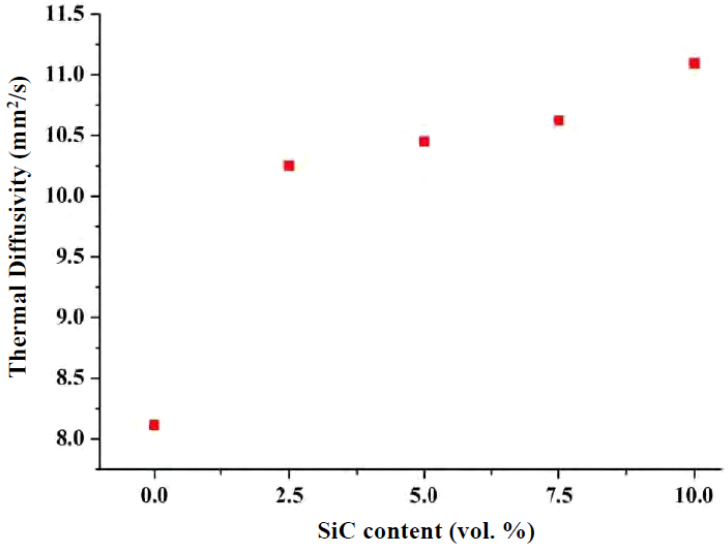

Figure 8. Change in the thermal diffusivity of SN based composites with SiC content at room temperature

In crystalline materials, thermal conductivity is provided by the phonon movement. The phonon movement is limited by the phonon mean free path in the structure [29]. With the increasing amount of SiC, SiC particles get closer and contact to each other. It is known that the termal conductivity of β-Si_3N_4 grains is higher in Si_3N_4 based ceramics [30]. Therefore, β-SiAlON grains formed in granule boundaries tought to be contributed on the increase in the thermal diffusivity.

The thermal diffusivity of investigated composites measured in the temperature range of 20-600°C are given in Figure 9.

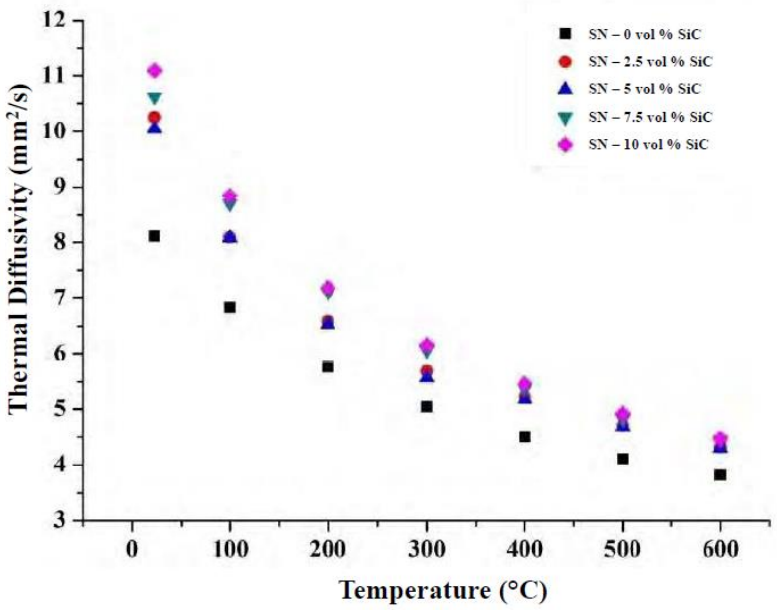

Figure 9. Change in the thermal diffusivity of SN based composites with SiC content at room temperature

4. CONCLUSION

Electrically and thermally conductive α/β SiAlON–SiC composites were produced by means of a segregated network concept. With the dry mixing process, spray dried SiAlON based granules (≤100_m) were coated with varying amounts of (up to 10 vol.%) nano SiC (75 nm) particles. All the composites and the reference SiAlON material were fully densified with gas pressure sintering at 1990°C under a N_2 gas pressure of 10 MPa. Microstructure and phase evolution and mechanical, electrical and thermal properties of the composites were studied and compared with the reference SiAlON material. The suppression of α→β SiAlON transformation by SiC was supported with microstructıral investigations. α/β SiAlON - 10 vol. % SiC composite had the highest hardness value (Hv_{10}: 16.33 GPa) due to the formation of α-SiAlON phases promoted with the increasing SiC content. No significant changes in the fracture toughness values of composites were observed. 3D segregated network of SiC particles along granules to establish electrical and thermal conductivity in the composites was successfully achieved with incorporation of 10 vol. % SiC α/β SiAlON - 10 vol. % SiC composite exhibited the semiconductor characteristic and high thermal conductivity with the electrical resistivity of 10^2 Ω.m and thermal diffusivity of ~11 mm^2/s measured at room temperature. The electrical resistivity values of the composites decreased with the increasing of SiC content. Thermal diffusivity values decreased with the increment of temperatures due to phonon-phonon scattering. No remarkable difference in thermal diffusivity values of SiC reinforced composites was noticed.

REFERENCES

[1] Riley F. Silicon nitride and related materials. J Am Ceram Soc 2000; 83: 245-265.

[2] Ayas E, Kara A, Kara F. A novel approach for preparing electrically conductive α/β SiAlON-TiN composites by spark plasma sintering. Journal of the Ceramic Society of Japan 2008; 116: 812-814.

[3] Bellosi A, Guicciardi S, Tampieri A. J Eur Ceram Soc 1992; 9: 83-93.

[4] Sawaguchi A, Toda K, Niihara K. J Am Ceram Soc 1991; 74: 1142-1144.

[5] Jiang D, Vleugels J, Van der Biest O, Liu W, Verheyen R, Lauwers B. Mater Sci Forum 2005; 492-493: 27-32.

[6] Jones AH, Trueman C, Dobedoe RS, Huddleston J, Lewis MH. British Ceramic Transactions 2001; 100: 49-54.

[7] Sciti D, Guicciardi S, Bellosi A. J Ceram Process Res 2002; 3: 87-95.

[8] Ayas E, Kara A, Kara F. α/β SiAlON based composites incorporated with $MoSi_2$ for electrical applications. In: Singh D, Zhu D, Zhou Y, editors. Design, Development and Applications of Engineering Ceramics and Composites. USA: Ceramic Transactions, 2010. pp. 189-195.

[9] Yurdakul H. Microstructural investigation of α-β SiAlON/SiC composites by analytical transmission electron microscopy. Journal of the Ceramic Society of Japan 2015; 123: 136-141.

[10] Liu Q, Gao L, Yan DS, Mandal H, Thompson DP. J Eur Ceram Soc 1997; 17: 593-598.

[11] Liu Q, Gao L, Yan DS, Mandal H, Thompson DP. J Eur Ceram Soc 1997; 17: 587-592.

[12] Bouchet J, Carrot C, Guillet J, Boiteux G, Seytre G, Pineri M. Conductive composites of UHMWPE and ceramics based on the segregated network concept. Poly Eng Sci 2000; 40: 36-45.

[13] Sandler JKW, Kirk JE, Kinloch IA, Shaffer MSP, Windle AH. Ultra-low electrical percolation threshold in carbon nanotube-epoxy composites. Polymer 2003; 44: 5893–5899.

[14] Carmona F. Conducting filled polymers. Physica A 1989; 157: 461–469.

[15] Kirkpatrick S. Percolation and conduction. Rev Mod Phys 1973; 45: 574-588.

[16] McLachlan DS, Blaszkiewicz M, Newnham RE. Electrical resistivity of composites. J Am Ceram Soc 1990; 73: 2187-2203.

[17] Kusy RP. Influence of particle size ratio on the continuity of aggregates. J Appl Phys 1977; 48: 5301-5305.

[18] Matsuo Y. Development of gas pressure sintered silicon nitride ceramics. In: Koizumi M, editor. Hot Isostatic Pressing-Theory and Applications. Netherlands: Springer Netherlands, 1992. pp. 49-54.

[19] Mandal H, Calis Acikbas N. SiAlON based functionally graded materials. In: Low IM, editor. Ceramic-Matrix Composites: Microstructure, Properties and Applications. Cambridge, England: Woodhead Publishing Limited and CRC press LLC, 2006. pp. 154-177.

[20] Mallik AK, Calis Acikbas N, Kara F, Mandal H, Basu D. A comparative study of SiAlON ceramics Ceramics International 2012; 38: 5757–5767.

[21] Kumar A, Mallik AK, Calis Acikbas N, Yaygıngol M, Kara F, Mandal H, Basu D, Biswas K, Basu B. Cytocompatibility property evaluation of gas pressure sintered SiAlON–SiC composites with

L929 fibroblast cells and Saos-2 osteoblast-like cells. Materials Science and Engineering C 2012; 32: 464-469.

[22] Kumar Mallik A, Madhav Reddy K, Calis Acikbas N, Kara F, Mandal H, Basu D, Basu B. Influence of SiC addition on tribological properties of SiAlON. Ceramics International 2011; 37: 2495–2504.

[23] Gazzara CP, Messier DR. Determination of phase content of Si_3N_4 by X-ray diffraction analysis. Ceram Bull 1977; 56: 777.

[24] Anstis GR, Chantikul P, Lawn BR, Marshall DB. A critical evaluation of indentation techniques for measuring fracture toughness: I, Direct Crack Measurements. J Am Ceram Soc 1981; 64: 533-538.

[25] Ayas E, Kara A. Novel electrically conductive α/β SiAlON/TiCN composites. Journal of the European Ceramic Society 2011; 31: 903–911.

[26] S. Hampshire, H.K. Park, D.P. Thompson, H.K. Jack, "α-SiAlON", Nature, 274 (1978) 880–882.

[27] Liu Q, Gao L, Yan DS, Thompson DP. Hard SiAlON ceramics reinforced with SiC nanoparticles. Mat Sci and Eng A 1999; 266: 1-7.

[28] Shackelford JF, Alexander W. Materials Science and Engineering Handbook. CRC Press LLC, 2001.

[29] Kushan SR. Investigation of the thermal conductivity of SiAlON ceramics (theses in Turkish with an abstract in English). PhD, Anadolu University, Eskişehir, Turkey, 2006.

[30] Hirao K, Watari K, Brito ME, Toriyama M, Kanzaki S. Hot isostatic pressing to increase thermal conductivity of Si_3N_4. J Am Ceram Soc 1996; 79: 2485-2488.